



# Origin of color variations of thin, nano-sized layers of volcanic cinder from the Sierra Negra Volcano of the Galapagos Islands

*Origen de las variaciones de color de las escorias del volcán Sierra Negra de las Islas Galápagos*

*Origem das variações de cores das escórias do vulcão Sierra Negra das Ilhas Galápagos*

Alexis Debut<sup>1</sup>, Theofilos Toulkeridis<sup>1,2</sup>, Andrea V. Vaca<sup>3</sup>, Carlos R. Arroyo<sup>1</sup>

Received: Nov/19/2020 • Accepted: Mar/9/2021 • Published: Jul/31/2021

## Abstract

Volcanic cinder, also known as scoria, is an extrusive igneous rock that forms when gas-rich magmas of basaltic or andesitic composition cool quickly. It is typically dark in color, ranging from black to red depending on its chemical composition. Sometimes fresh cinder samples show a variety of shiny metallic colors on its surface ranging from blue to gold to silver. The origin of these colors has remained unknown up to now. Cinder samples from an eruptive event occurred in October 2005 have been collected in the surroundings of the Sierra Negra volcano in the Galápagos Islands. The samples' crystallographic structure, chemical composition, and surface morphology have been analyzed using X-Ray diffractometry (XRD), energy dispersive X-Ray spectroscopy (EDS) and a field gun emission scanning electron microscopy (SEM), respectively. Based on an extensive physical and chemical analysis, we were able to demonstrate that these colors are due to a light interference phenomenon. These results have a great potential to be used for a wide variety of purposes such as determining the temperature and composition of magma and evaluating volcanic samples for planetary studies.

**Keywords:** Cinder; Galapagos; optical interference; nano-sized layers; crystallization speed; volcanology; diffraction

## Resumen

Las cenizas volcánicas, también conocidas como escorias, son una roca ígnea extrusiva que se forma cuando los magmas ricos en gas de composición basáltica o andesítica se enfrián rápidamente. Es típicamente de color oscuro, que va del negro al rojo dependiendo de su composición química. A veces las muestras de

Alexis Debut, [✉ apdebut@espe.edu.ec](mailto:apdebut@espe.edu.ec), [ID https://orcid.org/0000-0002-8269-7619](https://orcid.org/0000-0002-8269-7619)  
Theofilos Toulkeridis, [✉ ttoulkeridis@espe.edu.ec](mailto:ttoulkeridis@espe.edu.ec), [ID https://orcid.org/0000-0003-1903-7914](https://orcid.org/0000-0003-1903-7914)  
Andrea V. Vaca, [✉ andreav@lmmmp.mec.puc-rio.br](mailto:andreav@lmmmp.mec.puc-rio.br), [ID https://orcid.org/0000-0001-5066-6167](https://orcid.org/0000-0001-5066-6167)  
Carlos R. Arroyo, [✉ ccarroyo@espe.edu.ec](mailto:ccarroyo@espe.edu.ec), [ID https://orcid.org/0000-0002-1793-5799](https://orcid.org/0000-0002-1793-5799)

1 Universidad de las Fuerzas Armadas ESPE, Sangolquí, Ecuador.

2 Universidad de Especialidades Turísticas, Quito, Ecuador

3 Department of Mechanical Engineering, Pontifícia Universidade Católica do Rio de Janeiro, Rio de Janeiro, Brazil.



ceniza fresca muestran una variedad de colores metálicos brillantes en su superficie que van del azul al oro y a la plata, dependiendo de la orientación de la muestra. Hasta ahora, el origen de estos colores ha permanecido desconocido. Muestras de cenizas de un evento eruptivo ocurrido en octubre de 2005, han sido recogidas en los alrededores del volcán Sierra Negra en las Islas Galápagos. La estructura cristalográfica, la composición química y la morfología de la superficie de estas muestras se han analizado utilizando la difracción de rayos X (XRD), la espectroscopia de rayos X de dispersión de energía (EDS) y la microscopía electrónica de barrido con emisión de campo (SEM), respectivamente. Basándonos en un extenso análisis físico y químico, hemos podido demostrar que estos colores se deben a un fenómeno de interferencia de la luz. Estos resultados tienen un gran potencial para ser utilizados para una amplia variedad de propósitos como la determinación de la temperatura y la composición del magma, así como la evaluación de muestras volcánicas para estudios planetarios.

**Keywords:** Ceniza; Galápagos; interferencia óptica; capas de tamaño nano; velocidad de cristalización; vulcanología; difracción

## Resumo

As cinzas vulcânicas, também conhecidas como escórias, são uma rocha ígnea extrusiva formada quando os magmas ricos em gás de composição basáltica ou andesítico esfriam rapidamente. É tipicamente de cor escura, que vai do preto ao vermelho, dependendo de sua composição química. Às vezes as amostras de cinza fresca mostram uma variedade de cores metálicas brilhantes em sua superfície que vão do azul ao ouro e à cor prata, dependendo da orientação da amostra. Até o momento, a origem destas cores permanece desconhecida. Amostras de cinzas de um evento eruptivo ocorrido em outubro de 2005, foram recolhidas nos arredores do vulcão Sierra Negra nas Ilhas Galápagos. A estrutura cristalográfica, a composição química e a morfologia da superfície destas amostras foram analisadas por meio da difração de raios X (XRD), da espectroscopia de raios X por energia dispersiva (EDS) e da microscopia eletrônica de varredura com emissão de campo (SEM), respectivamente. Com base em uma extensa análise física e química, pudemos demonstrar que essas cores se devem a um fenômeno de interferência da luz. Esses resultados têm um grande potencial para serem utilizados com uma ampla variedade de propósitos como a determinação da temperatura e a composição do magma, bem como a avaliação de amostras vulcânicas para estudos planetários.

**Palavras-chave:** Cinza; Galápagos; interferência óptica; camadas de tamanho nano; velocidade de cristalização; vulcanologia; difração

## Introduction

Tephra or pyroclasts is one of the most easily accessible materials of active volcanoes, which may give fundamental clues about the eruptive state of the volcano (Fisher and Schmincke, 1984; Fisher, Heiken,

and Hulen, 1997; Schmid, 1981; White and Houghton, 2006). There is a variety of volcanic pyroclastic material which ranges in size from extremely fine ash, following by Pele's tears, and hair, lapilli, pumice rocks, cinder, reticulate, up to enormous blocks or bombs (Heiken, 1972; Peterson, 1979; Mangan and



Cashman, 1996; Moune, Faure, and Gauthier, 2007; Parfitt, 1998). These materials are formed during subaerial volcanic processes and they may be used for the analysis of volatile contents, degassing and crystallization as well as the prediction of further eruptive processes (Cashman, Sturtevant, and Papale, 2000; Toulkeridis, Arroyo, and Cruz D'Howitt, 2015). Additionally, the interaction of water with magma and other fragmentation processes can be studied by means of the shape, grain-size, glass or mineral content of the ejected pyroclastic material (Colgate and Sigurgeirsson, 1973; Spieler, Kennedy, and Kueppers, 2004; Wohletz, 1983; Zimanowski, Buettner, and Lorenz, 1997). Low-viscosity basaltic magmas form several types of close by located volcanic cones, such as scoria cones, tuff rings, tuff cones and maars, which are usually monogenetic and often associated or in the vicinity of shield volcanoes or stratovolcanoes (Lorenz, 1986; Vespermann and Schmincke, 2000; Wood, 1980). The study of terrestrial pyroclastic deposits may play also a fundamental role in the interpretation of the activity, development and also the origin of volcanic structures located in Mars, Venus and elsewhere among other remote space objects (Filiberto, 2017; Gail and Wilson, 2015; Hynek, McCollom, and Marcucci, 2013; Morris *et al.*, 2000; Squyres *et al.*, 2007).

The main aim of this study was to sample and characterize a variety of cinders of visually different shiny colors (Fig.1) with the goal to discover what factors produce them. The knowledge about the reactions and processes, which have led to the color variation of these materials, occurred in a well-known geologic context, can therefore serve to determine the conditions of volcanic deposits on Mars, Venus and elsewhere (Keszthelyi, Self, and Thordarson, 2006; McCanta, Dyar, and Treiman, 2014).

## Theoretical Framework

The Isabela Island situated on the western margin of the Galapagos is the largest island of the archipelago with an area of 4640 km<sup>2</sup>. This island has been partially formed at about a million of years ago by the subsequent joining of six shield volcanoes, being from north to south Ecuador, Wolf, Darwin, Alcedo, Sierra Negra and Cerro Azul (McBirney and Williams, 1969; Munro and Rowland, 1996). All of them are still active volcanoes and the eruptions of four of them have been reported in the last

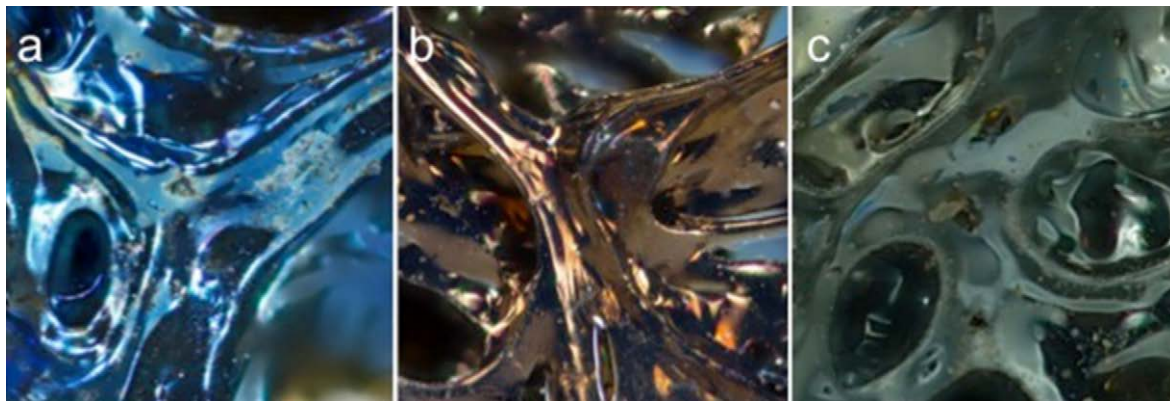


**Figure 1.** Three volcanic cinder showing visually different shiny metallic colors. (a) Blue, (b) Golden and (c) Silver



sixty years such as at Wolf in 1963, 1982 and 2015, Alcedo in 1993, Sierra Negra in 1963, 1979, 2005 and 2018 and Cerro Azul in 1959, 1979, 1998, and 2008 ([Global Volcanism Program, 2015](#); [Toulkeridis, 2011](#)).

The Sierra Negra volcano is a large active shield volcano, rising 1124 m above the sea level (m.a.s.l.), being situated at the south-east end of the Isabela Island in the Galapagos archipelago ([Geist et al., 2008](#); [McBirney and Williams, 1969](#); [Simkin, 1984](#); [Toulkeridis, 2011](#)). This voluminous shield volcano, like most others in this area, has been formed as a result of the Galapagos hotspot activity ([White, McBirney, and Duncan, 1993](#)). However, once the volcanoes have been transported away from the hotspot they become extinct, due to the ESE movement of the overlying Nazca oceanic plate relative to the South American and Caribbean continental plates, some 1000 km to the east ([Harpp and White, 2001](#); [Hey, 1977](#); [Holden and Dietz, 1972](#)). Sierra Negra has a width from 60 to 40 km and an elliptical caldera that measures from 7 to almost 10 km in diameter ([Amelung, Jónsson, and Zebker, 2000](#); [Reynolds, Geist, and Kurz, 1995](#)). It is the largest and simultaneously the second shallowest caldera of all volcanoes of the Galapagos Islands ([Chadwick and Howard, 1991](#); [White et al., 1993](#)). Its eruptive centers and different lava fields have been subdivided into seven distinctive age groups all being younger than 5000 years old ([Reynolds and Geist, 1995](#); [Reynolds et al., 1995](#); [Toulkeridis, 2011](#)). These centers produce from alkaline to tholeiitic basaltic lava flows that erupted from east to northeast trending by circumstantial and radial fissures situated on both sides of the summit caldera, on the upper flanks and on the western and eastern lower flanks ([Geist, Childs, and Scholl, 1988](#); [Kurz and Geist, 1999](#); [White et al., 1993](#)).

The caldera itself, which major axis strikes in an ENE-WSW direction, has undergone several episodes of collapse, upheaval and deformation up to recent times ([Amelung et al., 2000](#); [Chadwick, Geist, and Johnsson, 2006](#); [Geist, Chadwick, and Johnson, 2006](#); [Jonsson, Zebker, and Amelung, 2005](#); [Yun, Segall, and Zebker, 2006](#)). Particularly on the western side of the caldera floor inner parts of the caldera have been uplifted sub-parallel to the caldera rim, partially to altitudes higher than the caldera rim.

Ten historic eruptions occurred and some involved a frequently visited caldera rim fissure zone called “Volcán Chico” at the eastern outer margin of the caldera ([Delaney, Colony, and Gerlach, 1973](#); [Simkin and Siebert, 1994](#); [Toulkeridis, 2011](#)). These explosive phases of the past have given rise to frothy pumice, which was followed by the formation of agglutinate cones and voluminous lava flows. The former last volcanic event occurred in October 2005 when the volcano, after a repose of 26 years, erupted for about a week ([Geist et al., 2008](#)). During this event, approximately the twenty percent of the eastern caldera floor was covered, while a smaller part flowed outside the northern caldera rim (Fig. 2, [Geist et al., 2008](#)). A further most recent event occurred in 2018 ([Abe, Ohki, and Tadono, 2019](#)).

At present day, in the surroundings of Volcán Chico as well as at the western margin of an internal horst of the caldera floor there is an ongoing fumarolic activity, which is fault-controlled ([Goff, McMurtry, and Counce, 2000](#); [Goff and McMurtry, 2000](#); [Padrón, Hernández and Toulkeridis, 2012](#)). Four cinder samples corresponding to the eruption in October 2005 and showing predominant colors such as black, silver, golden and blue, were collected within a circular area of 1 km of radius centered at the major vent (Fig. 2). The GPS coordinates



and heights where the samples were collected were  $0^{\circ}46'45.89''S$   $91^{\circ}06'56.14''W$ , 993 m.a.s.l.,  $0^{\circ}46'55.57''S$   $91^{\circ}06'55.95''W$ , 1026 m.a.s.l.,  $0^{\circ}46'55.84''S$   $91^{\circ}06'43.35''W$ , 1018 m.a.s.l. and  $0^{\circ}46'45.22''S$   $91^{\circ}06'43.00''W$ , 965 m.a.s.l. respectively for the samples black, silver, golden and blue.

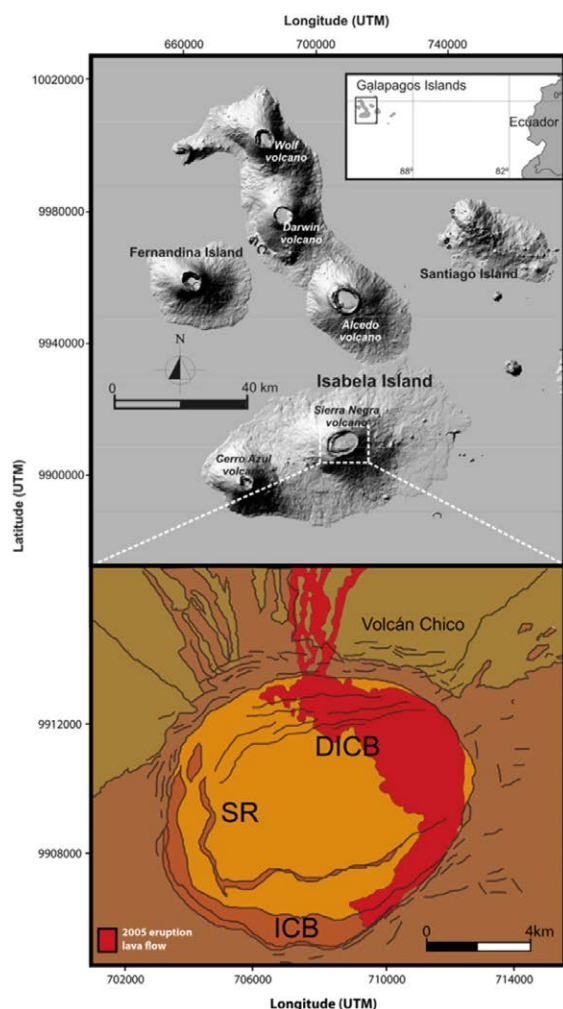


**Figure 2.** Above: Geographical location and shaded relief map of Sierra Negra volcano on Isabela Island, Galapagos archipelago. Below: Geologic map of the caldera of Sierra Negra Volcano with inter caldera bench (ICB), discontinuous inter caldera bench (DICB), sinuous ridge (SR), adapted from Reynolds and Geist (1995), Geist, Harpp and Naumann (2008) and Toulkeridis (2011).

## Methodology

The crystallographic structure and elemental chemical composition of the four different cinder samples above mentioned have been determined by X-Ray Diffractometry (XRD) and Energy-dispersive X-Ray Spectroscopy (EDS) respectively, whereas the morphology analysis has been performed by Scanning Electron Microscopy (SEM). The XRD has been carried out using an Empyrean diffractometer from PANalytical operating in a  $\theta$ - $2\theta$  configuration (Bragg-Brentano geometry) and equipped with a Cu X-ray tube ( $K\alpha$  radiation  $\lambda = 1.54056 \text{ \AA}$ ) operating at 40 kV and 40 mV.

The elemental analysis has been obtained by EDS which was performed on the SEM chamber at 30 kV using a Bruker X-Flash 6|30 detector, with a 123 eV resolution at Mn  $K\alpha$ . The morphological analysis has been elaborated using a Tescan Mira 3 microscope equipped with a Schottky Field Emission Gun (Schottky FEG-SEM) that allows us to obtain a resolution of 1.2 nm at 30 keV. Prior XRD and EDS measurements, we carefully scraped the sample surfaces and crushed them in a mortar adding acetone (EMSURE ®) in order to avoid the local heating that may induce phase changes in the material. For the XRD, the obtained powder has been deposited in a zero background XRD holder and for EDS the powder has been fixed in a stub previously covered with two layers of double coated carbon conductive tape. The morphological analysis of the surface of the samples has been performed by fixing small fragments of cinders of around  $0.125 \text{ cm}^3$  on SEM stubs and covering them with 20 nm of a conductive gold layer (99.99% purity) using a sputtering evaporator Quorum Q150R ES.



## Analysis and results

It is commonly accepted that the color of the cinders is originated by its chemical composition, however, there has not been any explanation or confirmation so far about the origin of its superficial shiny metallic colors. To clarify this issue, we have analyzed the surface of cinders of four visually different colors by using the XRD, EDS and SEM. Fig. 3 displays the XRD diffractograms obtained from the powder of cinders of four different colors. The XRD pattern do not illustrate clear peaks and the trends apparently appear to be similar for all encountered colors. Therefore, we concluded that the cinder samples do not indicate specific crystalline arrangement and there is no significant difference between different colors. The EDS measurements have been performed by considering the most common major elements represented in such volcanic samples, such as Na, Mg, Al, Si, K, Ca, Ti, Mn and Fe. In order to avoid biased determinations of the chemical compositions of the samples due to their inhomogeneity, we have averaged the spectra obtained from 10 points grid on a total

area of at least  $0.20 \text{ mm}^2$ . The presence of each element is denoted by the normalized weight percentage (norm. wt %), which is the percentage in weight, supposing that the chosen elements represent the total composition of the sample. We have neglected from the calculation the presence of C and O, for which the abundance in porous samples is higher than 50% (Goldstein, Newbury, and Echlin, 1992; Sánchez-Polo *et al.*, 2019). In order to compare the obtained EDS results, the norm. wt % average values of each element and the standard deviation are listed in Table 1. The table clearly indicates that there are no substantial differences in the chemical composition of cinders of different colors. Considering the obtained results from XRD and EDS analysis, we may conclude that the chemical composition is lacking to be the fundamental reason of the origin of the encountered and observed superficial metallic colors for these cinders.

That leads to the consideration, that the variation in the superficial colors may be due to a well-known optical phenomenon called thin-film interference (Knittl, 1976). In such kind of interference, the light waves reflect-

ed from the top and bottom boundaries of a thin film interfere with each other, either enhancing or reducing some colors in the reflected light. In order to confirm this assumption, several pictures of the surface of the cinders have been taken by the FEG-SEM (Fig. 4). There, the surface is composed of grains of different sizes, similar to nanocrystalline diamond films, which are grown by the Chemical Vapor Deposition (CVD) technique (Daenen, Williams, and D'Haen, 2006).

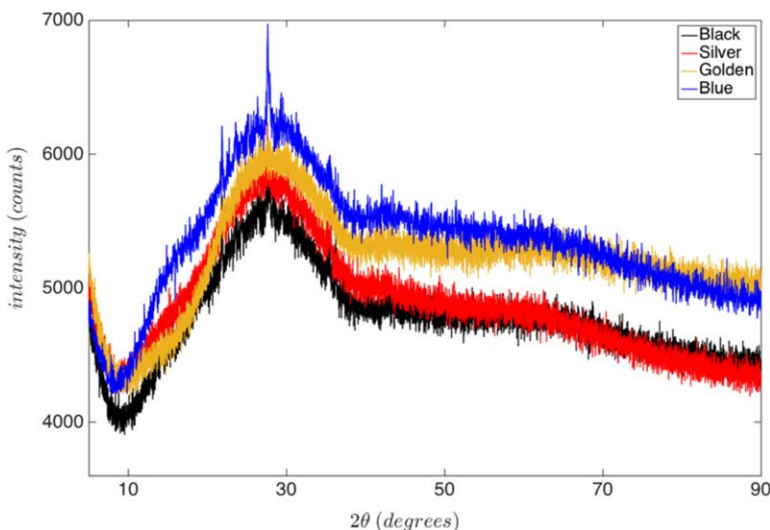


**Figure 3.** XRD patterns from Black, Silver, Golden and Blue cinder samples

**Table 1.** EDS measurements (norm. wt. %).

Norm. wt. (%)	Blue	Golden	Silver	Black
Na	6 ±1	6 ± 1	7 ±1	4 ±1
Mg	6 ±1	7 ±1	7 ±1	6 ±1
Al	13 ±1	12 ±2	13.3 ±0.4	12 ±1
Si	30 ±5	29 ±4	33 ±1	31 ±3
K	1.1 ±0.2	1.0 ±0.2	1.0 ±0.1	1.0 ±0.1
Ca	13 ±2	15 ±1	13 ±1	14 ±2
Ti	5 ±1	5 ±1	5 ±1	5 ±1
Mn	0.4 ±0.2	0.4 ±0.2	0.3 ±0.1	0.4 ±0.1
Fe	25 ±6	25 ±5	21 ±1	26 ±4

For each color, we have built a histogram based on an average of around 200 measurements. The histograms were built by taking the diameter of the circumscribed circle which determines the grain size as described

in (Arroyo, Debut, and Vaca, 2016). The mean values obtained for silver, golden and blue cinders have been  $180 \pm 60$  nm,  $150 \pm 40$  nm and  $100 \pm 40$  nm, respectively. Black color has no grain structure (Fig. 4 (d)), and therefore no special order of interference and color predominance. The growing process seems to be similar to the nucleation of random-oriented crystals as depicted by (Williams, 2011). By imaging a transversal cut of one of these cinders (Fig. 5), it is possible to observe that the grains are contained in a thin, nano-structured layer. The thickness of this layer has a similar size as the grain size, thus confirming our interference interpretation.

Based on the aforementioned results, we are able to justify about which is the source origin and magma behavior of the sampled cinders, knowing that their color is reflecting different stages of crystallization velocity and ejection speed. That means, cinder with blue color has crystallized faster than cinder with silver or golden colors, as reflected by their smaller grain sizes (Fig. 6). This observation may also serve in the general evaluation of a hazard area around an active volcano of such ejecting such pyroclasts and even the stability of such accumulated material (Jordá-Bordehore, Toulkeridis, and Romero-Crespo, 2016; Jordá-Bordehore and Toulkeridis, 2016).

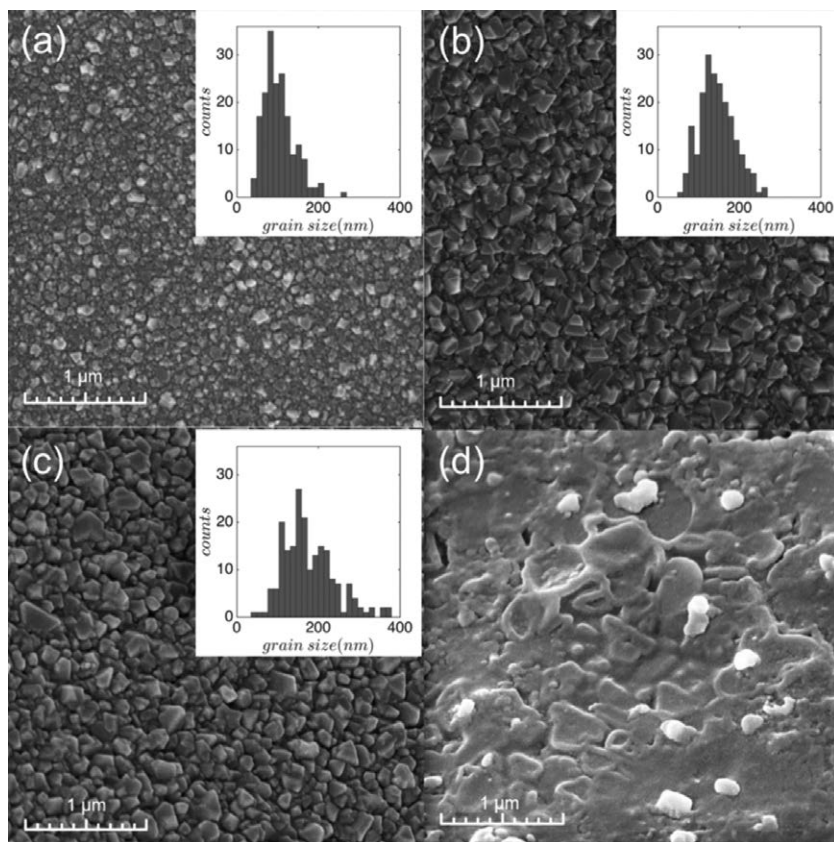


**Figure 4.** FEG-SEM pictures of the surface and grain size histograms taken at 10 kV for (a) Blue, (b) Golden, (c) Silver and (d) Black cinders.

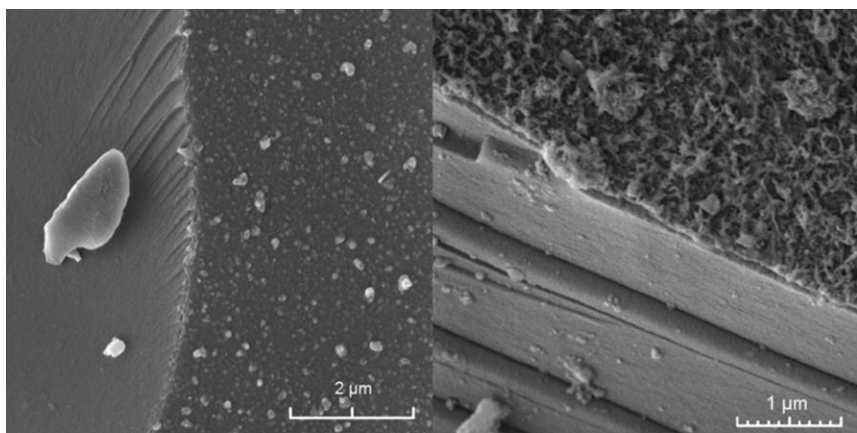


**Figure 5.** Sections of a cinder obtained by FEG-SEM at 10kV where one can observe a thin layer formed by grains



**Figure 6.** Color variations of cinder of the pyroclasts ejected on the surface of Sierra Negra volcano, Galapagos

Furthermore, similar to analogue studies of volcanic lava tubes and other volcanic environments or features on earth compared with other planets or moons (Keszthelyi, 1995; Keszthelyi *et al.*, 2006; Léveillé and Datta, 2010; Squyres *et al.*, 2007; Wilson and Head, 1994) or nanoparticles (Treichos E.M. *et al.*, 2021). The

obtained results may help to better characterize similar volcanic ejecta and their origin in other planetary environments, with similar or projected climate variations and subsequent conservation stages (Jakosky and Phillips, 2001; McCanta *et al.*, 2014; Morris *et al.*, 2000; Poulet, Bibring, and Mustard, 2005). Recent studies and associated observations on Mars within the Gusev crater have concluded on prominent parallel layering of accumulated pyroclastic materials, practical identical in appearance and chemical compositions to those pyroclasts of Sierra Negra volcano (Brož and Hauber, 2012). Such observations of Mars confirmed in a variety of studies the eruptive styles to be mainly effusive while having the resemblance of large shield volcanoes, with several volcanic cones, like cinder cones among others identical to those of Galapagos or Hawaii (Brož and Hauber, 2012; Ghent, Anderson, and Pithawala, 2012; Gulick and Baker, 1990). They also display shallow flanks, which were interpreted to be composed of pyroclastic deposits, mainly deposited by airfall (Brož and Hauber, 2012; Gregg and Farley, 2006; Kerber, Head, and Madeleine, 2011; Kerber, Head, and Madeleine, 2012).



## Conclusions

The unknown origin of the metallic shiny color of volcanic cinders has been revealed with a detailed analysis based on XRD, EDS and SEM measurements. The obtained results point out that the origin of the colors is a thin film interference effect. Furthermore, our findings reveal a lack of information about the chemical processes involved in the formation of the surface layer of cinders. Such studies on volcanic environments of hot spots are extremely useful in planetary studies with similar geodynamic settings and landscapes.

## Acknowledgements

The authors are grateful to Facundo Cabrera for the detailed images taking of the samples in his photographic laboratory. Sample permission has been given to TT by the Parque Nacional Galapagos based on the project No PC-05-04

## Conflict of Interest

The authors declare no competing interests.

## Author contribution statement

All the authors declare that the final version of this paper was read and approved.

The total contribution percentage for the conceptualization, preparation, and correction of this paper was as follows: A.D. 25 %., T.T. 25 %, A.V. 25% and C.R. 25 %.

## Data availability statement

The data supporting the results of this study will be made available by the corresponding author, **A.D.**, upon reasonable request.

## References

- Abe, T.; Ohki, M.; & Tadono, T. (2019). Surface Changes Due to the 2018 Eruption of Sierra Negra Volcano in Galápagos Island Revealed by ALOS-2/PALSAR-2. In *IGARSS 2019-2019 IEEE International Geoscience and Remote Sensing Symposium* (pp. 9334-9337). IEEE. <https://doi.org/10.1109/IGARSS.2019.8900424>
- Amelung, F.; Jónsson, S.; Zebker, H.; & Segall, P. (2000). Widespread uplift and ‘trapdoor’ faulting on Galapagos volcanoes observed with radar interferometry: *Nature*, 407: 993-996. <https://doi.org/10.1038/35039604>
- Arroyo, C. R.; Debut, A.; Vaca, A. V.; Stael, C.; Guzman, K.; & Cumbal, L. (2016). Reliable Tools for Quantifying the Morphological Properties at the Nanoscale. *Biology and Medicine*, 8(3), 1. <https://doi.org/10.4172/0974-8369.1000281>
- Brož, P.; & Hauber, E. (2012). A unique volcanic field in Tharsis, Mars: Pyroclastic cones as evidence for explosive eruptions. *Icarus*, 218(1), 88-99. <https://doi.org/10.1016/j.icarus.2011.11.030>
- Cashman, K. V.; Sturtevant, B.; Papale, P., & Navon, O. (2000). Magmatic fragmentation. In: Sigurdsson, H., Houghton, B.F., McNutt, S.R., Rymer, H., Stix, J. (Eds.), *Encyclopedia of Volcanoes*. Academic Press, San Diego, pp. 421-430.
- Chadwick, W.W.; Geist, D. J.; Johnsson, S.; Poland, M.; & Johnson, D. J. (2006). A volcano bursting at the seams: inflation, faulting, and eruption at Sierra Negra Volcano, Galápagos. *Geology*, 34, 1025-1028. <https://doi.org/10.1130/G22826A.1>
- Chadwick, W.W.; & Howard, K. A. (1991). The pattern of circumferential and radial eruptive fissures on the volcanoes of Fernandina and Isabela islands, Galápagos, *Bull. Volcanol.*, 53, 259-275. <https://doi.org/10.1007/BF00414523>
- Colgate, S. A.; & Sigurgeirsson, T. (1973). Dynamic mixing of water and lava. *Nature*, 244, 552-555. <https://doi.org/10.1038/244552a0>
- Daenen M.; Williams O. A.; D'Haen J.; Haenen K.; & Nesládek M. (2006). Seeding, growth and characterization of nanocrystalline diamond films on various substrates. *Phys. stat. sol.*, 203(12), 3005-3010. <https://doi.org/10.1002/pssa.200671122>



- Delaney, J. R.; Colony, W. E.; Gerlach, T. M; & Nordlie, B. E. (1973). Geology of the Volcan Chico area on Sierra Negra volcano, Galapagos Islands. *Geol Soc Am Bull*, 84, 2455-2470. [https://doi.org/10.1130/0016-7606\(1973\)84<2455:GTVCA>2.0.CO;2](https://doi.org/10.1130/0016-7606(1973)84<2455:GTVCA>2.0.CO;2)
- Filiberto, J. (2017). Geochemistry of Martian basalts with constraints on magma genesis. *Chemical Geology*, 466, 1-14. <https://doi.org/10.1016/j.chemgeo.2017.06.009>
- Fisher, R. V.; & Schmincke, H. U. (1984). "Pyroclastic Rocks". Springer-Verlag, Berlin/New York: pp. 472. <https://doi.org/10.1007/978-3-642-74864-6>
- Fisher, R. V.; Heiken, G.; & Hulen, J. B. (1997). *Volcanoes. Crucibles of Change*. Princeton Univ. Press, Princeton, NJ.
- Geist, D.J.; Chadwick, W.W. Jr.; & Johnson, D. J. (2006). Results from new GPS monitoring networks at Fernandina and Sierra Negra volcanoes, 2000-2002: *Journal of Volcanology and Geothermal Research*, 150, 79-97. <https://doi.org/10.1016/j.jvolgeores.2005.07.003>
- Geist, E. L.; Childs, J. R.; & Scholl, D. W. (1988). The origin of summit basins of the Aleutian Ridge: Implications for block rotation of an arc massif. *Tectonics*, 7(2), 327-341. <https://doi.org/10.1029/TC007i002p00327>
- Geist, D. J.; Harpp, K. S.; Naumann, T. R.; Poland, M.; Chadwick, W. W.; Hall, M.; & Rader, E. (2008). The 2005 eruption of Sierra Negra volcano, Galápagos, Ecuador. *Bulletin of Volcanology*, 70(6), 655-673. <https://doi.org/10.1007/s00445-007-0160-3>
- Ghail, R. C.; & Wilson, L. (2015). A pyroclastic flow deposit on Venus. *Geological Society, London, Special Publications*, 401(1), 97-106. <https://doi.org/10.1144/SP401.1>
- Ghent, R. R.; Anderson, S. W.; & Pithawala, T. M. (2012). The formation of small cones in Isidis Planitia, Mars through mobilization of pyroclastic surge deposits. *Icarus*, 217(1), 169-183. <https://doi.org/10.1016/j.icarus.2011.10.018>
- Global Volcanism Program (2015). Report on Wolf (Ecuador). In: Sennert, S.K. (ed.), *Weekly Volcanic Activity Report, 20 May-26 May 2015*. Smithsonian Institution and US Geological Survey
- Goff, F.; & McMurtry, G.M. (2000). Tritium and stable isotopes of magmatic waters. *Journal of Volcanology and Geothermal Research*, 97, 347-396. [https://doi.org/10.1016/S0377-0273\(99\)00177-8](https://doi.org/10.1016/S0377-0273(99)00177-8)
- Goff, F.; McMurtry, G.M.; Counce, D.; Simac, J.A.; Roldan-Manzo, A.R.; & Hilton, D.R. (2000). Contrasting hydrothermal activity at Sierra Negra and Alcedo volcanoes, Galapagos Archipelago, Ecuador. *Bull Volcanol*, 62, 34-52. <https://doi.org/10.1007/s004450050289>
- Goldstein J. I.; Newbury D. E.; Echlin P.; Joy D. C.; Romig A. D.; Lyman C. E.; Fiori C.; & Lifshin E. (1992). *Scanning Electron Microscopy and X-Ray Microanalysis*. A text book for Biologists, Materials Scientists, and Geologists. Springer-Verlag: Boston. <https://doi.org/10.1007/978-1-4613-0491-3>
- Gregg, T. K.; & Farley, M. A. (2006). Mafic pyroclastic flows at Tyrrhena Patera, Mars: Constraints from observations and models. *Journal of Volcanology and geothermal research*, 155(1-2), 81-89. <https://doi.org/10.1016/j.jvolgeores.2006.02.008>
- Gulick, V. C.; & Baker, V. R. (1990). Origin and evolution of valleys on Martian volcanoes. *Journal of Geophysical Research: Solid Earth*, 95(B9), 14325-14344. <https://doi.org/10.1029/JB095iB09p14325>
- Harpp, K. S.; & White, W. M. (2001). Tracing a mantle plume: Isotopic and trace element variations of Galápagos seamounts. *Geochemistry, Geophysics, Geosystems*, 2(6). <https://doi.org/10.1029/2000GC000137>
- Heiken, G. (1972). Morphology and petrography of volcanic ashes. *Geological Society of America Bulletin*, 83(7), 1961-1988. [https://doi.org/10.1130/0016-7606\(1972\)83\[1961:MAPOVA\]2.0.CO;2](https://doi.org/10.1130/0016-7606(1972)83[1961:MAPOVA]2.0.CO;2)
- Hey, R. (1977). Tectonic evolution of the Cocos-Nazca spreading center. *Geological Society of America Bulletin*, 88, 1404-1420. [https://doi.org/10.1130/0016-7606\(1977\)88<1404:TEOTCS>2.0.CO;2](https://doi.org/10.1130/0016-7606(1977)88<1404:TEOTCS>2.0.CO;2)
- Holden, J. C.; & Dietz, R. S. (1972). Galápagos Gore, NazCoPac Triple Junction and Carnegie/Cocos Ridges. *Nature*, 235, 266-269. <https://doi.org/10.1038/235266a0>
- Hynek, B. M.; McCollom, T. M.; Marcucci, E. C.; Brugman, K.; & Rogers, K. L. (2013). Assessment of environmental controls on acid-sulfate alteration at active volcanoes in



- Nicaragua: Applications to relic hydrothermal systems on Mars. *Journal of Geophysical Research: Planets*, 118(10), 2083-2104. <https://doi.org/10.1002/jgre.20140>
- Jakosky, B. M.; & Phillips, R. J. (2001). Mars' volatile and climate history. *Nature*, 412(6843), 237. <https://doi.org/10.1038/35084184>
- Jonsson, S; Zebker, H; & Amelung, F. (2005). On trapdoor faulting at Sierra Negra volcano, Galapagos. *J Volcanol Geotherm Res*, 144, 59-71. <https://doi.org/10.1016/j.jvolgeores.2004.11.029>
- Jordá-Bordehore, L.; & Toulkeridis, T. (2016). Stability assessment of volcanic natural caves - Lava tunnels - Using both empirical and numerical approach, case studies of galapagos islands (Ecuador) and lanzarote Island (Canary - Spain). Rock Mechanics and Rock Engineering: From the Past to the Future. International Symposium on International Society for Rock Mechanics, ISRM 2016; Cappadocia; Turkey, 2, 835-840.
- Jordá-Bordehore, L.; Toulkeridis, T.; Romero-Crespo, P.L.; Jordá-Bordehore, R.; & García-Garriazabal, I. (2016). Stability assessment of volcanic lava tubes in the Galápagos using engineering rock mass classifications and by empirical approach. International *Journal of Rock Mechanics & Mining Sciences*, 89, 55-67. <https://doi.org/10.1016/j.ijrmms.2016.08.005>
- Kerber, L.; Head, J. W.; Madeleine, J. B.; Forget, F.; & Wilson, L. (2011). The dispersal of pyroclasts from Apollinaris Patera, Mars: Implications for the origin of the Medusae Fossae Formation. *Icarus*, 216(1), 212-220. <https://doi.org/10.1016/j.icarus.2011.07.035>
- Kerber, L.; Head, J. W.; Madeleine, J. B.; Forget, F.; & Wilson, L. (2012). The dispersal of pyroclasts from ancient explosive volcanoes on Mars: Implications for the friable layered deposits. *Icarus*, 219(1), 358-381. <https://doi.org/10.1016/j.icarus.2012.03.016>
- Keszthelyi, L. (1995). A preliminary thermal budget for lava tubes on the Earth and planets. *Journal of Geophysical Research: Solid Earth*, 100(B10), 20411-20420. <https://doi.org/10.1029/95JB01965>
- Keszthelyi, L.; Self, S.; & Thordarson, T. (2006). Flood lavas on earth, Io and Mars. *Journal of the geological society*, 163(2), 253-264. <https://doi.org/10.1144/0016-764904-503>
- Knittl, Z. (1976). *Optics of thin films: an optical multilayer theory* (p. 548) London: Wiley.
- Kurz, M. D.; & Geist, D. (1999). Dynamics of the Galapagos hotspot from helium isotope geochemistry. *Geochimica et Cosmochimica Acta*, 63(23), 4139-4156. [https://doi.org/10.1016/S0016-7037\(99\)00314-2](https://doi.org/10.1016/S0016-7037(99)00314-2)
- Léveillé, R. J.; & Datta, S. (2010). Lava tubes and basaltic caves as astrobiological targets on Earth and Mars: a review. *Planetary and Space Science*, 58(4), 592-598. <https://doi.org/10.1016/j.pss.2009.06.004>
- Lorenz, V. (1986). On the growth of maars and diatremes and its relevance to the formation of tuff rings. *Bull. Volcanol*, 48, 265-274. <https://doi.org/10.1007/BF01081755>
- Mangan, M. T.; & Cashman, K. V. (1996). The structure of basaltic scoria and reticulite and inferences for vesiculation, foam formation, and fragmentation in lava fountains. *Journal of Volcanology and Geothermal Research*, 73(1), 1-18. [https://doi.org/10.1016/0377-0273\(96\)00018-2](https://doi.org/10.1016/0377-0273(96)00018-2)
- McBirney, A. R.; & Williams, H. (1969). Geology and petrology of the Galápagos Islands: *Geological Society of America Memoir* 118. <https://doi.org/10.1130/MEM118-p1>
- McCanta, M. C.; Dyar, M. D.; & Treiman, A. H. (2014). Alteration of Hawaiian basalts under sulfur-rich conditions: Applications to understanding surface-atmosphere interactions on Mars and Venus. *American Mineralogist*, 99(2-3), 291-302. <https://doi.org/10.2138/am.2014.4584>
- Morris, R. V.; Golden, D. C.; Bell, J. F.; Sheller, T. D.; Scheinost, A. C.; Hinman, N. W.; Furniss, G.; Mertzman, S.A.; Bishop, J.L.; Ming, D.W.; Allen, C.C.; & Britt, D.T. (2000). Mineralogy, composition, and alteration of Mars Pathfinder rocks and soils: Evidence from multispectral, elemental, and magnetic data on terrestrial analogue, SNC meteorite, and Pathfinder samples. *Journal of Geophysical Research: Planets*, 105(E1), 1757-1817. <https://doi.org/10.1029/1999JE001059>
- Moune, S.; Faure, F.; Gauthier, P. J.; & Sims, K. W. (2007). Pele's hairs and tears: natural probe of volcanic plume. *Journal of volcanology and geothermal research*, 164(4), 244-253. <https://doi.org/10.1016/j.jvolgeores.2007.05.007>



- Munro, D. C.; & Rowland, S. K. (1996). Caldera morphology in the western Galapagos and implications for volcano eruptive behavior and mechanisms of caldera formation. *Journal of Volcanology and Geothermal Research*, 72(1-2), 85-100. [https://doi.org/10.1016/0377-0273\(95\)00076-3](https://doi.org/10.1016/0377-0273(95)00076-3)
- Padrón, E.; Hernández, P.A.; Pérez, N.M.; Toulkeridis, T.; Melián, G.; Barrancos, J.; Virgili, G.; Sumino H.; & Notsu, K. (2012) Fumarole/plume and diffuse CO<sub>2</sub> emission from Sierra Negra volcano, Galapagos archipelago. *Bull. Of Volcanol.*, 74, 1509-1519. <https://doi.org/10.1007/s00445-012-0610-4>
- Parfitt, E. A. (1998). A study of clast size distribution, ash deposition and fragmentation in a Hawaiian-style volcanic eruption. *Journal of Volcanology and Geothermal Research*, 84(3), 197-208. [https://doi.org/10.1016/S0377-0273\(98\)00042-0](https://doi.org/10.1016/S0377-0273(98)00042-0)
- Peterson, D. W. (1979). Significance of the flattening of pumice fragments in ash-flow tuffs. *Geological Society of America Special Papers*, 180, 195-204. <https://doi.org/10.1130/SPE180-p195>
- Poulet, F.; Bibring, J. P.; Mustard, J. F.; & Gendrin, A. (2005). Phyllosilicates on Mars and implications for early Martian climate. *Nature*, 438(7068), 623. <https://doi.org/10.1038/nature04274>
- Reynolds, R.W.; Geist, D.; & Kurz, M.D. (1995). Physical volcanology and structural development of Sierra Negra volcano, Isabela Island, Galapagos Archipelago. *Geol Soc Am Bull*, 107, 1398-1410. [https://doi.org/10.1130/0016-7606\(1995\)107<1398:P-VASDO>2.3.CO;2](https://doi.org/10.1130/0016-7606(1995)107<1398:P-VASDO>2.3.CO;2)
- Reynolds, R.W.; & Geist, D.J. (1995). Petrology of lavas from Sierra Negra volcano, Isabela Island, Galapagos Archipelago. *J Geophys Res*, 100(24), 537-524,553. <https://doi.org/10.1029/95JB02809>
- Sánchez-Polo, A.; Briceño, S.; Jamett, A.; Galeas, S.; Campaña, O.; Guerrero, V.; Arroyo, C.R.; Debut, A.; Mowbray, D.J.; Zamora-Ledezma, C.; Serrano, J. (2019). An Archaeometric Characterization of Ecuadorian Pottery. *Sci Rep*, 9, 2642. <https://doi.org/10.1038/s41598-018-38293-w>
- Schmid, R. (1981). Descriptive nomenclature and classification of pyroclastic deposits and fragments: Recommendations of the IUGS Subcommission on the Systematics of Igneous Rocks. *Geology*, 9(1), 41-43. [https://doi.org/10.1130/0091-7613\(1981\)9<41:D-NACOP>2.0.CO;2](https://doi.org/10.1130/0091-7613(1981)9<41:D-NACOP>2.0.CO;2)
- Simkin, T. (1984). *Geology of Galapagos Islands*. In: Perry R (ed) Galapagos. Pergamon Press, Oxford, pp 15-41
- Simkin, T.; & Siebert, L. (1994). *Volcanoes of the World: A Regional Directory, Gazetteer, and Chronology of Volcanism During the Last 10,000 Years*. 349 pp. Geosci. Press, Tucson, Ariz.
- Spieler, O.; Kennedy, B.; Kueppers, U.; Dingwell, D. B.; Scheu, B.; & Taddeucci, J. (2004). The fragmentation threshold of pyroclastic rocks. *Earth and Planetary Science Letters*, 226(1), 139-148. <https://doi.org/10.1016/j.epsl.2004.07.016>
- Squyres, S. W.; Aharonson, O.; Clark, B. C.; Cohen, B. A.; Crumpler, L.; De Souza, P. A.; Farrand, W.H.; Gellert, R.; Grant, J.; Grotzinger, J.P.; Haldemann, A.F.C.; Johnson, J.R.; Klingelhoefer, G.; Lewis, K.W.; Li, R.; McCoy T.; McEwen, A.S.; McSween, H.Y.; Ming, D.W.; Moore, J.M.; Morris, R.V.; Parker, T.J.; Rice, Jr. J.W.; Ruff, S.; Schmidt, M.; Schröder, C.; Soderblom, L.A.; & Yen, A. (2007). Pyroclastic activity at home plate in Gusev Crater, Mars. *Science*, 316(5825), 738-742. <https://doi.org/10.1126/science.1139045>
- Toulkeridis, T. (2011). *Volcanic Galápagos Volcánico*. Ediecuatorial, Quito, Ecuador: 364pp.
- Toulkeridis, T.; Arroyo, C. R.; Cruz D'Howitt, M.; Debut, A.; Vaca, A. V.; Cumbal, L.; Mato, F.; & Aguilera, E. (2015). Evaluation of the initial stage of the reactivated Cotopaxi volcano-analysis of the first ejected fine-grained material. *Natural Hazards and Earth System Sciences Discussions*, 3, 6947-6976. <https://doi.org/10.5194/nhessd-3-6947-2015>
- Trejos E.M., Silva L.F.O., Hower J.C., Flores E.M.M., González C.M., Pachón J.E., Aristizábal B.H. (2021). Volcanic emissions and atmospheric pollution: A study of nanoparticles. *Geosciences Frontiers*, 12(2), 746-755.
- Vespermann, D.; & Schmincke, H.-U. (2000). Scoria cones and tuff rings. In: Sigurdsson, H., Houghton, B.F., McNutt, S.R., Rymer, H., Stix, J. (Eds.), *Encyclopedia of Volcanoes*. Academic Press, San Diego, pp. 683-694.
- White, J. D. L.; & Houghton, B. F. (2006). Primary volcanioclastic rocks. *Geology*, 34(8), 677-680. <https://doi.org/10.1130/G22346.1>



- White, W. M.; Mc Birney, A. R.; & Duncan, R. A. (1993). Petrology and geochemistry of the Galápagos Islands: Portrait of a pathological mantle plume. *Journal of Geophysical Research: Solid Earth*, 98(B11), 19533-19563. <https://doi.org/10.1029/93JB02018>
- Williams O.A. (2011). Nanocrystalline diamond: Diamond & Related Materials, Elsevier. 20, 621-640. <https://doi.org/10.1016/j.diamond.2011.02.015>
- Wilson, L.; & Head, J. W. (1994). Mars: Review and analysis of volcanic eruption theory and relationships to observed landforms. *Reviews of Geophysics*, 32(3), 221-263. <https://doi.org/10.1029/94RG01113>
- Wohletz, K. H. (1983). Mechanisms of hydrovolcanic pyroclast formation: Grain size, scanning electron microscopy, and experimental results. *J. Volcanol. Geotherm. Res.*, 17, 31-63. [https://doi.org/10.1016/0377-0273\(83\)90061-6](https://doi.org/10.1016/0377-0273(83)90061-6)
- Wood, C. A. (1980). Morphometric evolution of cinder cones. *J. Volcanol. Geotherm. Res.*, 7, 387-413. [https://doi.org/10.1016/0377-0273\(80\)90040-2](https://doi.org/10.1016/0377-0273(80)90040-2)
- Yun, S.-H.; Segall, P.; & Zebker, H.A. (2006). Constraints on magma chamber geometry at Sierra Negra Volcano, Galápagos Islands, based on InSAR observations. *Journal of Volcanology and Geothermal Research*, 150, 232-243. <https://doi.org/10.1016/j.jvolgeores.2005.07.009>
- Zimanowski, B.; Buettner, R.; Lorenz, V.; & Haefele, H.-G. (1997). Fragmentation of basaltic melt in the course of explosive volcanism. *J. Geophys. Res.* 102, 803-814. <https://doi.org/10.1029/96JB02935>



Origin of color variations of thin, nano-sized layers of volcanic cinder from the Sierra Negra Volcano of the Galapagos Islands (Alexis Debut • Theofilos Toulkeridis • Andrea V. Vaca• Carlos R. Arroyo) [Uniciencia](#) is protected by [Attribution-NonCommercial-NoDerivs 3.0 Unported \(CC BY-NC-ND 3.0\)](#)